Luminescence Properties and Energy Transfer of Eu^{2+} Doped $Ca_8Mg(SiO_4)_4Cl_2$ Phosphors

Xiao Zhang and Xingren Liu

Changchun Institute of Physics, Academia Sinica, Changchun 130021, Jilin, China

ABSTRACT

The synthesis and luminescence characteristics of Eu^{2+} activated calcium magnesium chlorosilicate, $Ca_8Mg(SiO_4)_4Cl_2$, have been reported and analyzed. The emission spectrum of Eu^{2+} is composed of two separate bands with peaks at 507 and 428 nm, which result from the Eu^{2+} centers in different crystallographic sites. At room temperature, the excitation spectrum of the very strong 507 nm emission shows not only the broad $4f^7$-$4f^65d$ excitation bands, but also the fine structure resulting from the splitting of $4f^6$ configuration in the $4f^65d$ excited state. This structure is explained by the high covalency degree of the cation—anion bonds in this system. Efficient energy transfer between the two inequivalent Eu^{2+} centers has been evaluated quantitatively.

The luminescence of Eu^{2+} activated phosphors usually results from the ground $4f^7(^8S_{7/2})$ level to the $4f^65d$ excited configuration, and, therefore has a broad band character that depends strongly on the nature of the host lattice. The emission color of Eu^{2+} can vary in a broad range from ultraviolet to red. Since the 4f-5d transition is an allowed electrostatic dipole transition, the absorption and emission of Eu^{2+} are very efficiency in many hosts, which makes the Eu^{2+} doped phosphors of practical importance in fluorescent and duplication lamps. In an octahedral site, the absorption of Eu^{2+} arises from the crystal field split e_g and t_{2g} states of a $4f^65d$ configuration, which can be further split when the site symmetry becomes lower.

For the host lattices which have more than one crystallographic site available for divalent europium ions, the energy transfer usually takes place between the inequivalent Eu^{2+} centers. This phenomenon has been observed by many researchers (1-3), and was discussed by Blasse *et al.* (4-6). These authors have shown that the energy transfer occurs even at a very low concentration, owing to the parity allowed transition of Eu^{2+}. For example, the critical energy transfer distance in a Rb_2ZnBr_4: Eu system is about 35 Å (4).

In this paper, the synthesis and spectral properties of divalent europium ions in a new calcium magnesium chlorosilicate hosts, $Ca_8Mg(SiO_4)_4Cl_2$, with a cubic crystal structure, are reported and discussed. The luminescence of Eu^{2+} appears as two broad bands due to the different centers in inequivalent crystal sites. The energy transfer between the two kinds of Eu^{2+} ions is observed and evaluated quantitatively, which gives a critical transfer distance of 25 Å.

Structure Description

The luminescence host of calcium magnesium chlorosilicate, $Ca_8Mg(SiO_4)_4Cl_2$, has a cubic crystal structure with space group of Fd3m (7). The unit cell parameter a = 15.06 Å. There are eight formula units involved in one unit cell, and the stereostructure of the atom arrangement in an unsymmetric unit is illustrated in Fig. 1. In the crystal lattices, there exist three kinds of cation sites; two Ca sites and one Mg site. The crystal field environments for the three sites are very different. Ca atoms occupy both an octahedral site with six oxygen nearest neighbors and a polyhedral site surrounded by six oxygen and two chlorine atoms, which are named as Ca(I) and Ca(II) sites, respectively. As to the Ca(I) site, besides the six nearest oxygen neighbors, there are also six chlorine atoms at the next nearest anion positions at a distance of about 5Å, which will influence the crystal field at Ca(I) site through nephelauxetic and covalent effects. Therefore, this site may have a pseudo-12-coordination character. The site symmetry for Ca(I) is C_{2V}, whereas that for Ca(II) is C_1. According to the crystal structure given in Ref. 7, the site ratio of Ca(I) against Ca(II) is 1:3. Mg atoms occupy a position of regular tetrahedral symmetry with four oxygen ligands at an identical distance of 1.86 Å. This character is very special in the crystal structure of silicate materials, and results from the cooperative polarization of magnesium by nearest oxygen and next nearest chlorine atoms. As a consequence of the polarization effect, the covalency of the Mg-O ionic bond increases considerably. In other words, the ionic polarization from chlorine atoms disturbs the bonding orbitals of magnesium and oxygen atoms, which makes the two ions bond by the uniform sp^3 hybridized orbitals to get regular Mg-O tetrahedral structure. In addition, most of the bonds of cation and anion are covalent intermediate bonds, which makes the structure very stable. The distance between nearest Ca(II) and Mg is about 3.25 Å, and that between Ca(I) and Ca(II) is 3.73 Å.

Experimental

The powder polycrystal sample of $Ca_8Mg(SiO_4)_4Cl_2$ was synthesized by a high temperature reaction. The starting materials of $CaCO_3$, MgO, SiO_2, and $CaCl_2$ of reagent grade were mixed together by a mole ratio of $CaCO_3$:MgO:SiO_2:$CaCl_2$ = 7:1:4:1.5. A small amount of high purity Eu_2O_3 replacing $CaCO_3$ was added in the mixture. The well mixed raw materials were fired at 1000-1150°C for 2-4 h in a reduc-

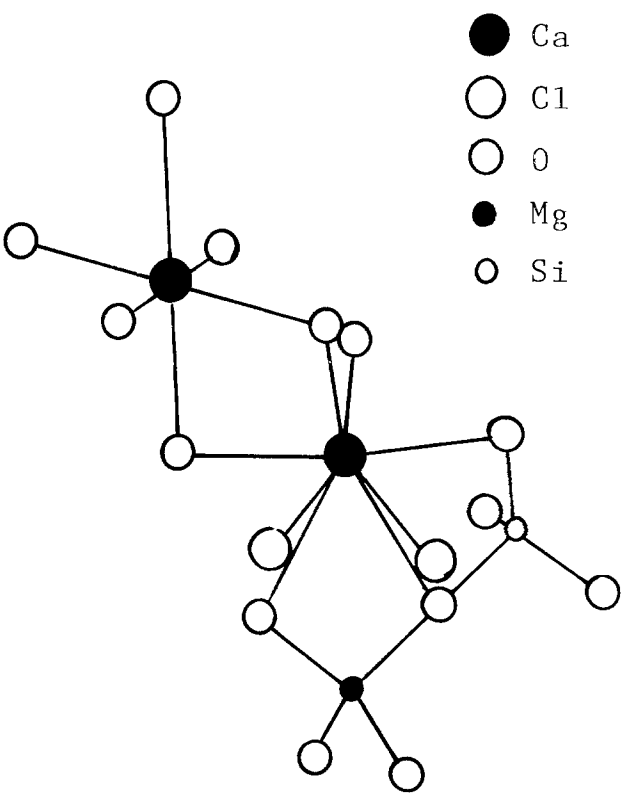

Fig. 1. Stereostructure of atom arrangement in an unsymmetric unit.

ing atmosphere. The product was then washed with deionic water to remove the extra $CaCl_2$ and other water soluble components.

The crystal structure of the sample was checked using a D/Max-rA x-ray diffractometer, and the diffraction pattern was in excellent agreement with that reported earlier (7). This indicates that the products in this study are cubic $Ca_8Mg(SiO_4)_4Cl_2$. Emission and excitation spectra were measured using a Hitachi MPF-4 spectrofluorimeter equipped with a microcomputer in correcting the energy distribution of light source and the responding sensitivity of photomultiplier. A 75 W xenon lamp was used as the excitation lamp. All the measurements were performed at room temperature. The luminescence decay of Eu^{2+} was measured at liquid nitrogen temperature, 77 K, using a double-beam Spex-1403 spectrometer. A 337.1 nm N_2 pulse laser was used as the excitation source. The signal from the spectrometer was introduced into the 162/165 boxcar integrator and then processing datamate, the decay curve was plotted by the on-line plotter.

Results and Discussion

Optical spectra.—The Eu^{2+} activated $Ca_8Mg(SiO_4)_4Cl_2$ compounds are efficient green emission phosphors under either ultraviolet or blue light excitation. The emission spectra of Eu^{2+} in $Ca_8Mg(SiO_4)_4Cl_2$: 0.1 Eu with different excitation wavelengths of 330 (a), 380 (b), and 490 nm (c) are shown in Fig. 2. The emission spectra are similar upon different excitation wavelengths. With ultraviolet light excitation, the spectrum consists of both a very strong green band with a peak at 507 nm and a half width of 56 nm, and a weak blue band with maximum at about 428 nm. These two bands are due to the Eu^{2+} ions in different crystal sites; the strong 507 nm band is assigned to Eu(II), and the weak 428 nm band is ascribed to Eu(I).

The excitation spectrum for 507 nm emission band is depicted in Fig. 3. The very broad excitation spectrum extending from 220 to 500 nm mainly has two characters. Several broad bands are due to the parity allowed $4f^7$ ($^8S_{7/2}$)-$4f^65d$ transitions: the subband with peak at about 250 nm is due to the ground $^8S_{7/2}$ to crystal field split e_g ($4f^65d$) state, the ones at 350, 375 and 430 nm vicinities are corresponding to the t_{2g} ($4f^65d$) state. In addition, fine structure is observed on the low energetic excitation

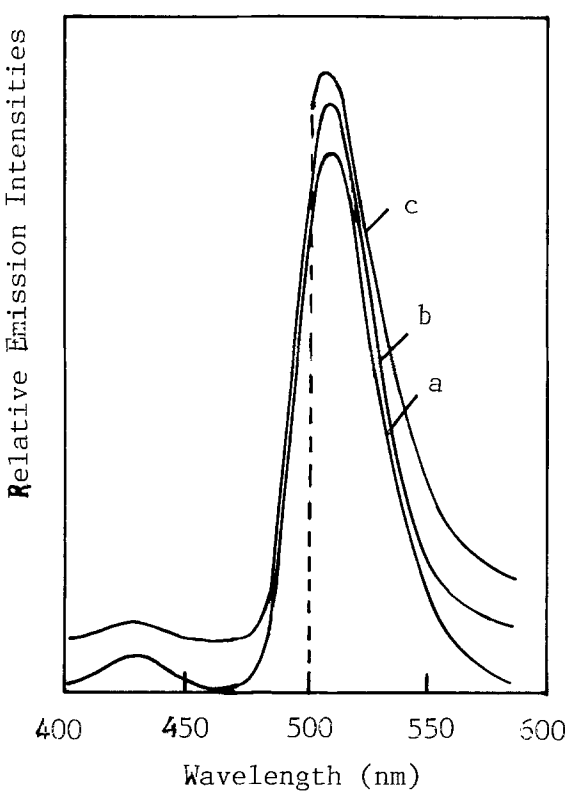

Fig. 2. Emission spectra of $Ca_8Mg(SiO_4)_4Cl_2$:0.1Eu with excitation into 330 (a), 380 (b) and 490 nm (c).

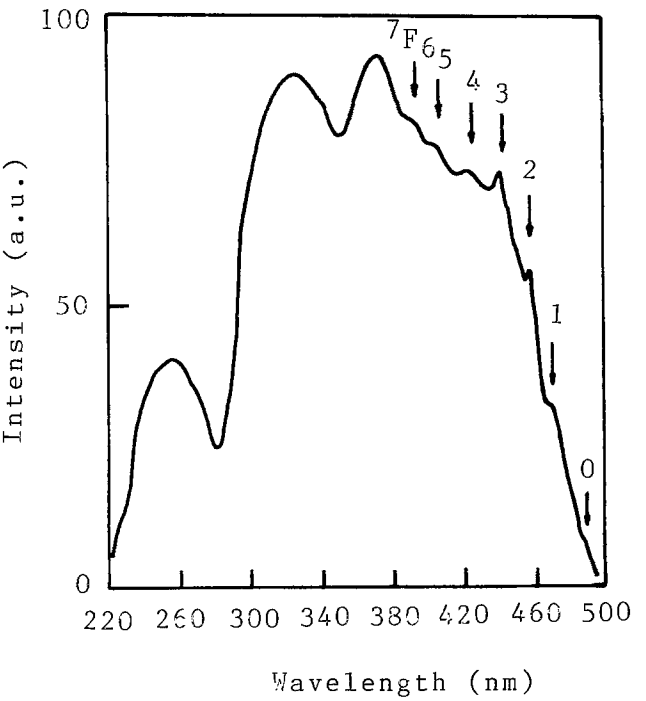

Fig. 3. Excitation spectrum of Eu^{2+} 507 nm emission in $Ca_8Mg(SiO_4)_4Cl_2$:0.1Eu. The arrows indicate the positions from Eu^{3+} ground levels.

bands, which can be resolved at room temperature. This fine structure is assigned to the splitting of the $4f^6$ configuration in the $4f^65d$ excited state into seven ^7F_J levels. Ryan *et al.* had suggested that the appearance of this structure is possible when the exchange interaction between the six 4f electrons and the 5d electron is small (8). The energy intervals are in good agreement with the result obtained from ground state splitting of Eu^{3+} ions. A comparison between the theoretical values and the experiment results is given in Table I. The arrows in Fig. 3 represent the relative positions obtained by the energy level diagram of Eu^{3+} ion (12), which coincide with the experimental curve. This character has also been reported by several authors in other systems at 1.8 and 4.2 K (5-6, 8-9). Contrary to nonstructure excitation spectrum, the fine structure in which the position of the lowest excited level $4f^6(^7F_0)5d$ can be determined accurately makes the precise determination of the Stokes shift of Eu^{2+} possible. From the results represented in Fig. 2 and 3, the Stokes shift in this system gives a value of 600 cm^{-1}, which is much smaller than the result obtained from broad band excitation.

The excitation spectrum of the weak band is depicted in Fig. 4. In contrast to Fig. 3, the vibrational fine structure is not observed. The two excitation bands at 280 and 360 nm correspond to the ground $^8S_{7/2}$ to the e_g and t_{2g} states of $4f^65d$ configuration. Compared with Fig. 3, the halfwidths for the two bands are much smaller. The $^8S_{7/2}$-e_g band has no apparent fine structures, and the one from the transition of $^8S_{7/8}$ to t_{2g} shows three overlapped subbands with very small spacing. Referring to the excitation subband at 370 nm, the Stokes shift for this center emission is about 3700 cm^{-1}.

Table I. Comparison of theoretical and experimental results of $Eu^{2+}{}^8S_{7/2} - 4f^6(^7F_J)$ 5d transitions in $Ca_8Mg(SiO_4)_4Cl_2$ host.

Terminal level	Experimental		Theoretical[12]		ΔE (cm^{-1})
	λ(nm)	E(cm^{-1})	λ(nm)	E(cm^{-1})	
$^7F_0$	492	20325	492	20325	—
$^7F_1$	481	20790	483	20700	90
$^7F_2$	466	21459	466	21441	18
$^7F_3$	448	22231	449	22282	−51
$^7F_4$	427	23419	428	23388	39
$^7F_5$	407	24570	410	24390	180
$^7F_6$	393	25445	394	25396	49

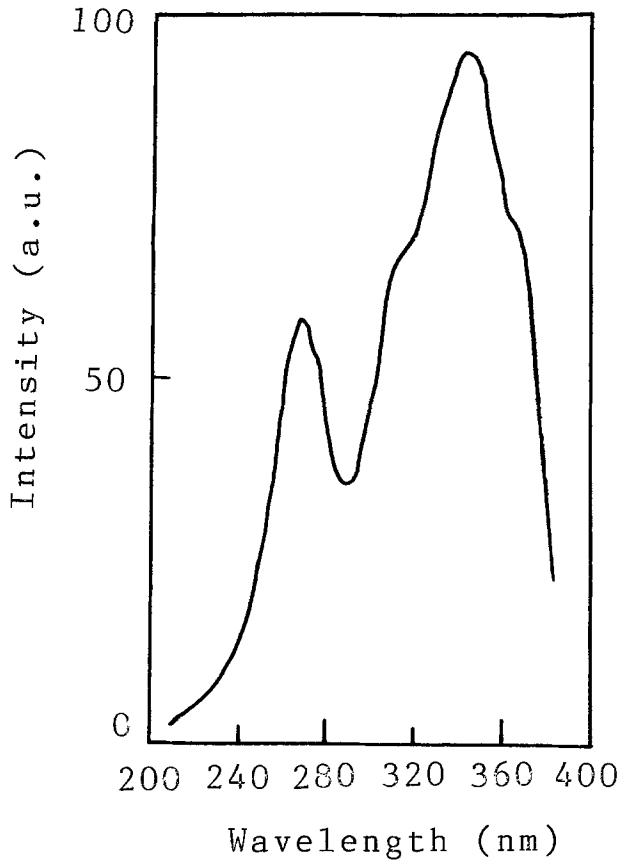

Fig. 4. Excitation spectrum of Eu^{2+} 428 nm emission in the same sample as Fig. 3.

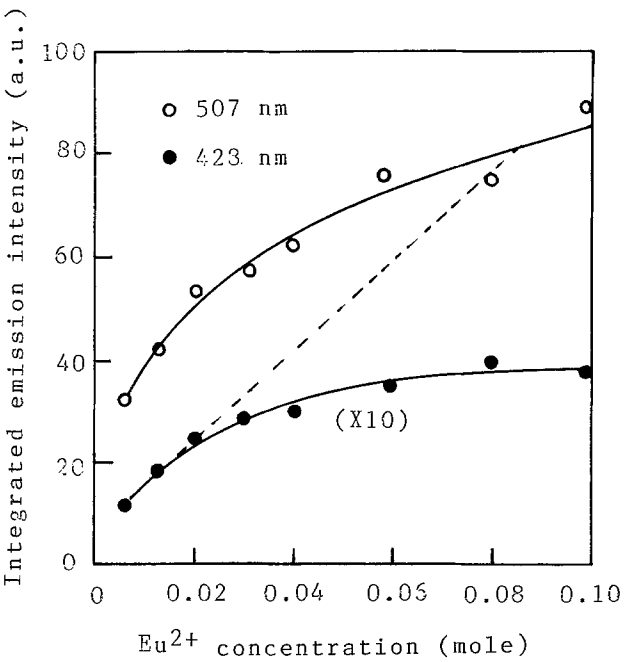

Fig. 5. Dependence of Eu^{2+} integral emission intensities as a function of concentrations for excitation at 330 nm.

From the crystal structure described above, these two excitation spectra can be interpreted accordingly. For the Eu(I) site, which refers to Eu^{2+} ion in Ca(I) position and surrounded by six oxygen atoms in an identical spacing of 2.36 Å, the site symmetry is nearly an octahedral one with small distortion so that the 5d orbitals degenerate into two parts as e_g and t_{2g} levels with no further splitting. Whereas for Eu(II) site, the eight-coordinated position with C_1 site symmetry, the site environment deviates from an octahedron remarkably, therefore, the split e_g and t_{2g} levels are further split by the lower site symmetry, which makes the energy levels complicated and the excitation bands broaden. It is worth stating that the nephelauxetic and covalent effects from chlorines at next nearest anion sites to Ca(I) will weaken the crystal field at Ca(I) sites. The crystal field splitting of the $4f^65d$ level of Eu^{2+}(I) will become smaller, which will shift the lowest $4f^65d$ state to higher energies. As a result, both the excitation and emission bands are situated at shorter wavelengths. This is probably the reason that the 6-coordinated Eu(I) gives rise to a shorter wavelength emission band than the 8-coordinated Eu(II). The fluorescence lifetime for the 507 nm emission band is about 0.5 μs, which does not change much with increasing concentration. This result is in accordance with the change of emission intensity, see Fig. 5, which implies that the concentration quenching is small. The fluorescence lifetime for 428 nm emission is difficult to measure correctly, owing to the very weak emission.

Ryan *et al.* (8) have pointed out that the weak exchange interaction of the $4f^6$ and 5d electrons is responsible for the existence of ^7F_J splitting from the $4f^65d$ configuration. The exchange interaction is dependent on the degree of localization of the 5d electron near the Eu^{2+} core. This localization has a strong relation with the degree of covalency present in the interaction of the 5d electron with surrounding coordinates. For the $Ca_8Mg(SiO_4)_4Cl_2$ host, most of the cation-anion are linked via covalent intermediate bonds, the degree of covalency is much higher than in ionic crystals and, therefore, the exchange interaction between six 4f electrons and 5d electron becomes very weak. This weak interaction makes the ^7F_J splitting from $4f^6$ configuration observed and well resolved at room temperature.

As predicted from the crystal structure, the population of Eu^{2+} in Ca(I) site is much less than that in Ca(II) site. Figure 5 shows the dependence of relative emission intensities of Eu(I) and Eu(II) centers on the Eu^{2+} concentrations. Both emission intensities increase with increasing concentration at lower activator contents, and the ratio between intensities of the two emission bands is nearly constant at a value of about 0.04. At higher Eu^{2+} concentrations, the luminescence of Eu(I) is quenched. This probably results from the energy transfer from Eu(I) to Eu(II).

Energy transfer.—The $4f^7$-$4f^65d$ transition of Eu^{2+} is an allowed electric dipole transition, so that energy transfer from Eu(I) to Eu(II) will occur via electric dipole-dipole interaction. Due to the good spectral overlap between the Eu(I) emission band and the Eu(II) excitation bands, the energy transfer between these two inequivalent Eu^{2+} centers is expected to be very efficient. Unfortunately, the fluorescence decay characteristics of the Eu(I) center is difficult to measure accurately owing to the limited population of this center. For energy transfer between inorganic ions via electric dipole-dipole interaction, the critical distance of energy transfer according to the well known Forster-Dexter multipolar interaction theory (10, 11), can be expressed as (13)

$$R_C^6 = 0.63 \times 10^{28} \frac{4.8 \times 10^{-16} \cdot P}{E^4} \cdot SO$$

Here P is the oscillator strength of activator ion, SO is the spectral overlap integral, and E is the energy at the maximum spectral overlap. For an Eu^{2+} $4f^7$-$4f^6(^7F_J)$ 5d absorption band, P is taken as 0.01, according to the result given by Meijerink *et al.* (5). From Eu(I) emission and Eu(II) excitation spectrum, the spectral overlap integral, SO, is estimated at about 1.0 eV^{-1}. With these values, the critical distance for energy transfer in this system is calculated at about 25 Å.

Assuming all of the europium ions, which are added as Eu_2O_3, enter the $Ca_8Mg(SiO_4)_4Cl_2$ and Eu^{2+} in Ca(I) and Ca(II) positions, neglecting the concentration quenching of the luminescence from Eu(I) center, which is reasonable since the distribution coefficient of Eu(I) center is small, the integral emission intensity of Eu(I) ions should be proportional to the doping concentration of Eu^{2+}. According

to the result represented in Fig. 5, the critical concentration X_C, which is regarded as the concentration at which the actual emission intensity is about 1/2 of the value from the proportional line, is 0.07 mol.

The critical distance for energy transfer can be calculated from X_c using the equation (13)

$$R_C = 2\left(\frac{3V}{4\pi N X_c}\right)^{1/3}$$

where V is the unit cell volume and N is the number of molecules in a unit cell. For $Ca_8Mg(SiO_4)_4Cl_2$ host, V is equal to 3419.3 Å^3 and N equals 8. This gives a critical distance of 23 Å. This result is in good agreement with that obtained using the Forster-Dexter theory. This reveals that the Eu(I)-Eu(II) energy transfer is very efficient.

Conclusion

This paper has shown that Eu^{2+} activated $Ca_8Mg(SiO_4)_4Cl_2$ is an efficient green emission phosphor under both UV and blue light excitation, and that the two crystallographic sites for Eu^{2+} in this host give rise to different spectroscopic behavior. The excitation spectrum of Eu(II) center shows a fine structure of the splitting of $4f^65d$ excited state into seven ^7F_J levels, which can be resolved even at room temperature. This phenomenon has been interpreted by the high covalency degree of the anion-cation bonds in $Ca_8Mg(SiO_4)_4Cl_2$ lattices. The fine structure gives an opportunity in determinating the lowest excited $4f^6(^7F_0)$ 5d level, which consequently makes a precise determination of the Stokes shift possible. The Stokes shift for Eu(II) emission in this system is about 600 cm^{-1}, which is much smaller than that reported in literature for the broad band excitation spectrum and is comparable with the result for similar condition given by Meijerink (5). The analysis of Eu(I) center emission gives rise to a Stokes shift of about 3700 cm^{-1}.

Energy transfer between the two inequivalent Eu^{2+} centers has been discussed. From the relative emission intensity and the Forster-Dexter theory, the critical energy transfer distance has been calculated. The results in these two approaches are in good agreement. The obtained critical distance is about 25 Å, which reveals that the energy transfer in this system is very efficient.

Acknowledgment

The authors are indebted to Professor Yu Baogui and Ms. Guan Zhengsu for measuring optical spectra. This work is supported by The Applied Research Foundation of JiLin Privince, China.

REFERENCES

1. G. Blasse, *Phys. Status Solidi B*, **55**, K131 (1973).
2. J. T. C. Van Kemenade and G. P. F. Hoeks, Electrochem. Soc. Spring Meeting 1983, San Francisco, Ext. Abstr. 607.
3. M. Leskela, T. Koskentalo, and G. Blasse, *J. Sol. Stat. Chem.*, **59**, 272 (1985).
4. G. Blasse, *ibid.*, **62**, 207 (1986).
5. A. Meijerink and G. Blasse, *J. Lumin.*, **43**, 283 (1989).
6. A. Meijerink, J. Nuyten, and G. Blasse, *ibid.*, **44**, 19 (1989).
7. Ruilen Ye, Xinrong Wang, and Zheying Zhang, *J. Chinese Ceram. Soc.*, **15**, 309 (1987).
8. F. M. Ryan, W. Lehman, D. W. Feldman, and J. Murphy, *This Journal*, **121**, 1475 (1974).
9. A. Meijerink and G. Blasse, *J. Lumin.*, **47**, 1 (1990).
10. Th. Forster, *Ann. Phys.*, **2**, 55 (1948).
11. D. L. Dexter, *J. Chem. Phys.*, **21**, 836 (1953).
12. G. H. Dieke, in "Spectra and Energy Levels of Rare Earth Ions in Crystal," H. M. Crosswhite and H. Crosswhite, Editors, p. 248 (1968).
13. G. Blasse, *Philips Res. Repts.*, **24**, 131 (1969).

Comparison of Single and Tri-Layer Technologies for Volume Production of Sub-Half Micron Gate GaAs MESFETs

T. Hwang,[1] G. W. Wang, Y. Chang, and C. L. Lau

Ford Microelectronics, Incorporated, Colorado Springs, Colorado 80921-3698

ABSTRACT

Both single and trilayer technologies have been evaluated for the production of sub-half micron gate-length devices on 3-in. diameter GaAs substrates using deep ultra-violet photolithography. The trilayer technique is capable of fabricating 0.4 μm gate-length devices with yields exceeding 86%. However, the single layer process has the advantages of fabricating 0.5 μm gate-length devices with greater simplicity, reduced cost, and east of rework. The improved gate resolution and yield of the trilayer process are attributed to the very thin top layer resist, planarized surface, and the reactive ion etching in process. The trilayer process also has the potential for fabricating 0.25 μm gate-length devices with good uniformity and high yield. We compare dc and microwave characteristics of devices fabricated with both single and trilayer techniques. These data indicate no device degradation resulting from the more complicated trilayer process.

Although GaAs monolithic microwave integrated circuits (MMICs) offer the advantages of reduced size, higher reliability, and broader bandwidth, one of the major obstacles for inserting these circuits into systems is their high cost of fabrication. Therefore, a high volume and high yield manufacturing process is essential to the success of GaAs MMIC technology. Despite the recent advances of high electron mobility transistors (HEMTs) and heterojunction bipolar transistors (HBTs), ion implanted GaAs MESFETs remain the industry's workhorse due to their greater ease of fabrication. In order to improve MESFET performance and extend their applications to millimeter-wave frequencies, the gate length must be reduced to dimensions less than one-half of a micron (1-2).

As gate length decreases, standard photolithography becomes increasingly difficult and limits products yield and throughput. E-beam direct-write lithography is routinely used for submicron applications. However, because of its high capital cost and extremely low throughput, E-beam lithography is mainly a research tool.

Optical photolithographies with single and multilayer resist techniques have been used to fabricate sub-half micron gates on GaAs MESFETs (3-5). These processes were performed on 2 in. diameter GaAs wafers with yelds less than 50% for 0.25 μm gate-length devices. In this study, we compare single and trilayer processes for the fabrication of 0.25-0.50 μm gate features. Eleven lots, containing a total of thirty-two wafers, were used for this evaluation. In addition to the yield and gate length uniformity, the resolution capability of both processes is reported.

[1] Present address: AVANTEK, 3175 Bowers Avenue, Santa Clara, California 95054-3292.